

# Environmental Science Nano

Accepted Manuscript



This is an *Accepted Manuscript*, which has been through the Royal Society of Chemistry peer review process and has been accepted for publication.

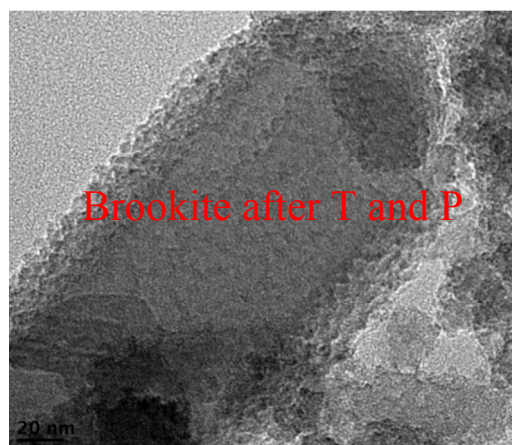
*Accepted Manuscripts* are published online shortly after acceptance, before technical editing, formatting and proof reading. Using this free service, authors can make their results available to the community, in citable form, before we publish the edited article. We will replace this *Accepted Manuscript* with the edited and formatted *Advance Article* as soon as it is available.

You can find more information about *Accepted Manuscripts* in the [Information for Authors](#).

Please note that technical editing may introduce minor changes to the text and/or graphics, which may alter content. The journal's standard [Terms & Conditions](#) and the [Ethical guidelines](#) still apply. In no event shall the Royal Society of Chemistry be held responsible for any errors or omissions in this *Accepted Manuscript* or any consequences arising from the use of any information it contains.

TOC

Polymorph-dependent titanium dioxide nanoparticle dissolution in acidic and alkali digestions



## Nano impact

Titanium dioxide nanoparticles are used in a variety of domestic products including paints, plastics, inks, food colorings, toothpastes, cosmetics and sun-screens. Furthermore,  $\text{TiO}_2$  is one of the most widely used photocatalysts for water and air purification, and is used as a coating for self-cleaning surfaces and other environmental cleaning purposes. Recently,  $\text{TiO}_2$  has been reclassified as a group 2B carcinogen, “possibly carcinogenic to humans”, by the International Agency for Research on Cancer. The specific characteristics of various types of  $\text{TiO}_2$  nanoparticles and their potential impacts on human health and ecosystems have resulted in a need for further research on the quantification of different polymorphs of  $\text{TiO}_2$  nanoparticles in the environment. The present study investigates the digestibility of different polymorphs of  $\text{TiO}_2$ -nanoparticles using MW-based  $\text{HF}/\text{HNO}_3$  mixed acid digestion and MF-based KOH alkaline fusion methods. The main goal of the present study is to compare the dissolution efficacy of different  $\text{TiO}_2$  nanoparticles polymorphs in different environmental matrix using established MW-based HF mixed acid digestion and modified MF-based KOH fusion. The environmental matrices encompassed stream bed sediments, kaolinite and bentonite.

1 **Polymorph-dependent titanium dioxide nanoparticle dissolution in acidic and alkali**  
2 **digestions**

3

4 R. G. Silva<sup>1\*</sup>, M. N. Nadagouda<sup>2</sup>, C. L. Patterson<sup>2</sup>, Srinivas Panguluri<sup>1</sup>, T. P. Luxton<sup>2</sup>, E. Sahle-  
5 Demessie<sup>2</sup>, C. A. Impellitteri<sup>2</sup>

6 <sup>1</sup> CB&I Federal Services LLC, 1600 Gest Street, U.S. EPA Test and Evaluation Facility,  
7 Cincinnati OH 45204, USA

8 <sup>2</sup>United States Environmental Protection Agency, National Risk Management Research  
9 Laboratory, Cincinnati, OH 46268, USA

10

11

12 \*Corresponding Author

13 <sup>1</sup> CB&I Federal Services LLC, 1600 Gest Street, U.S. EPA Test and Evaluation Facility,  
14 Cincinnati OH 45204, USA

15

16

17

18

19

20

21

22

23

## 1 Abstract

2 Multiple polymorphs (anatase, brookite and rutile) of titanium dioxide nanoparticles (TiO<sub>2</sub>-NPs)  
3 with variable structures were quantified in environmental matrices via microwave-based  
4 hydrofluoric (HF) and nitric (HNO<sub>3</sub>) mixed acid digestion and muffle furnace (MF)-based  
5 potassium hydroxide (KOH) fusion. The environmental matrices included stream bed sediments,  
6 kaolinite and bentonite. The percentage of Titanium (Ti) recovered from the mixed acid  
7 digestion was not statistically different from KOH fusion when anatase and brookite TiO<sub>2</sub>-NPs  
8 were blended in all three environmental matrices. However, the percentage of Ti recovery of  
9 rutile TiO<sub>2</sub>-polymorph from the samples digested using mixed acid digestion method was  
10 significantly lower [23 (±5), 12 (±6), 11 (±0.6)] than those digested using KOH fusion method  
11 [74 (±4), 53 (±7), 75 (±2)]. The recovery percent values reported are for Ti in sediments,  
12 kaolinite and bentonite, matrices respectively. Exposing the TiO<sub>2</sub>-NP spiked samples to elevated  
13 heat and pressure reduced the recovery of Ti from all three polymorphs via mixed acid digestion.  
14 In contrast, Ti recoveries from KOH fusion improved after heat and pressure treatment. A  
15 narrowing of the X-ray diffraction (XRD) peaks for anatase and brookite after heat and pressure  
16 treatment indicated an increase in the aggregation or particle interaction of the TiO<sub>2</sub>-NPs. The  
17 XRD peaks for rutile TiO<sub>2</sub>-NP polymorph was similar before and after heat and pressure  
18 treatment. In summary, regardless of the selected environmental matrix type, the mixed acid  
19 digestibility of TiO<sub>2</sub>-NPs is polymorph-dependent; whereas, the KOH-fusion digestibility is  
20 polymorph independent. Therefore, when analyzing environmental samples containing TiO<sub>2</sub>-  
21 NPs with unknown polymorphs, a KOH-fusion digestion method is recommended for yielding  
22 consistent results.

23

## 1 **Keywords**

2 Titanium dioxide; nanoparticles; temperature effects, particle structure

3

## 4 **Introduction**

5

6 Titanium dioxide nanoparticles (TiO<sub>2</sub>-NPs) are used in various domestic products including  
7 paints, plastics, inks, food colorings, toothpastes, cosmetics and sun-screens.<sup>1-3</sup> Additionally,  
8 TiO<sub>2</sub> is one of the most widely used photocatalysts for water and air purification, and is used as a  
9 coating for self-cleaning surfaces and other environmental cleaning purposes.<sup>1-5</sup> For example,  
10 anatase TiO<sub>2</sub> is used in ultraviolet light (UV,  $\lambda < 397$  nm) photocatalysis for generating hydroxyl  
11 radicals which can inactivate microbes and degrade a variety of organic compounds.<sup>6</sup> It has also  
12 been reported that TiO<sub>2</sub> photocatalysts exhibit reactivity under visible light (Vis,  $\lambda > 400$  nm)  
13 even under the low illumination of interior lighting.<sup>6</sup> Thus, in the presence of both UV and Vis  
14 light, photo-reactive species of TiO<sub>2</sub> can be a concern if released into the environment. Recently,  
15 TiO<sub>2</sub> has been reclassified as a group 2B carcinogen, “possibly carcinogenic to humans”, by the  
16 International Agency for Research on Cancer.<sup>7</sup> The specific characteristics of various types of  
17 TiO<sub>2</sub>-NPs and their potential impacts on human health and ecosystems have resulted in a need  
18 for further research on the quantification of different polymorphs of TiO<sub>2</sub>-NPs in the  
19 environment. Polymorphism is a condition in which a solid chemical compound exists in more  
20 than one crystalline form. These forms differ in physical and chemical properties resulting  
21 different stability and bioavailability.<sup>8</sup> These polymorphic differences are commonly captured  
22 using X-ray diffraction (XRD) patterns but not every environmental research study performs  
23 XRD analysis.

1  
2 Microwave (MW)-based hydrofluoric (HF)/nitric (HNO<sub>3</sub>) mixed acid and alkaline fusion are the  
3 most effective methods for quantifying refractory metals such as Ti.<sup>9-15</sup> Although methods  
4 involving HF as a single acid digestion are atypical, MW-based HF mixed acid digestion results  
5 in greater metal recovery. In addition, the application of HF is required for the complete  
6 digestion and quantification of refractory metals in geological and environmental sample  
7 matrices such as soil, sediments and dusts.<sup>16-17</sup> This is because HF dissolves the aluminosilicate  
8 structure of environmental materials and facilitates the liberation of metals.<sup>8,18</sup> However, a  
9 recent study,<sup>13</sup> reported that Ti recovery by alkaline fusion using lithium metaborate (LiBO<sub>2</sub>)  
10 was greater than open-vessel HF mixed acid digestion for rutile-rich environmental samples.  
11 Taylor et al,<sup>17</sup> also reported that the alkaline fusion method was superior to the closed-vessel  
12 MW-based acid digestion procedure in determining refractory metals such as Ti. There are other  
13 studies to support the superiority of the alkaline fusion method over HF digestion for dissolution  
14 of refractory mineral containing samples.<sup>18</sup> Thus, there is still some ambiguity about the  
15 effectiveness of digestion procedures in spite of a huge amount of research that has been  
16 completed on dissolution and determination of refractory metals in environmental samples. The  
17 variety of mineral polymorphs make the digestion methodology and quantification in the sample  
18 of interest a challenge.<sup>8</sup> For example, refractory metal Ti has several naturally occurring  
19 polymorphs such as anatase, brookite and rutile with different structures, surface enthalpy and  
20 stability.<sup>19-20</sup> Generally, the thermodynamic stability is in this order: rutile > brookite >  
21 anatase.<sup>21</sup> However, the thermodynamic stability is particle size dependent. At the nano-scale,  
22 anatase is more stable than rutile, but rutile becomes the more stable as particle-size increases.<sup>22</sup>  
23 Despite known differences in size-dependent thermodynamic stability, literature concerning the

1 digestion techniques for Ti dissolution and quantification of TiO<sub>2</sub>-NP polymorphs is minimal.  
2 Most of the existing studies are usually based on the general Ti containing environmental  
3 samples.<sup>13,17</sup> The growing demand for TiO<sub>2</sub>-NPs for various products and processes has, resulted  
4 in the generation of other polymorphs of TiO<sub>2</sub>-NPs, which are required to be quantified in the  
5 environmental samples.

6  
7 In addition to the aforementioned polymorph-and size-dependent thermodynamic stabilities  
8 impacting the Ti recovery, the Ti recovery can be altered due to the chemical reaction between  
9 Ti and other sample matrix elements during sample processing in the heat range of 160-260°C.<sup>19-</sup>  
10 <sup>24</sup> For example, Ti reacts with different calcium and aluminum-bearing compounds during the  
11 sample digestion process in the aforementioned heat range.<sup>24</sup> The degree of the reaction is  
12 substantial on the surface of particles during the digestion process.<sup>23</sup> During digestion, a film  
13 may form on the surface of TiO<sub>2</sub>-NPs in the presence of caustic potash altering the metal  
14 extraction rate.<sup>20,25</sup> Thus, the release of Ti from TiO<sub>2</sub>-NPs may vary based on the surface  
15 properties of different TiO<sub>2</sub>-NP polymorphs regardless of the digestion procedure.

16  
17 In a previous paper, we have reported the accuracy and precision of Muffle-furnace (MF)-based  
18 fusion compared to traditional Bunsen burner-based fusion in determining Ti from different  
19 polymorphs of TiO<sub>2</sub> NPs.<sup>26</sup> In this paper, we further investigate the digestibility of different  
20 polymorphs of TiO<sub>2</sub>-NPs using MW-based HF/HNO<sub>3</sub> mixed acid digestion and MF-based KOH  
21 alkaline fusion methods. The main goal of the present study is to compare the dissolution  
22 efficacy of different TiO<sub>2</sub>-NP polymorphs using established MW-based HF mixed acid digestion  
23 and modified MF-based KOH fusion. Bulk degradation methods are very important for initial



1 risk assessment in environmental samples. Dependable initial screening procedures for total Ti  
2 can aid risk assessors in determining whether or not to pursue more detailed chemical speciation  
3 data for a particular sample or site. The impact of heat and pressure on TiO<sub>2</sub>-NP  
4 stability/reactivity and subsequent Ti recovery from TiO<sub>2</sub>-NPs (pure and blended in  
5 environmental materials) was the secondary objective of this study.

6

## 7 **Experimental Methods and Procedures**

8

### 9 **TiO<sub>2</sub>-NPs types and characterization**

10

11 The detailed experimental protocols are discussed in a prior study.<sup>26</sup> The three TiO<sub>2</sub>-NP  
12 polymorphs studied in this study were anatase, brookite and rutile. The anatase TiO<sub>2</sub>-NPs were  
13 obtained from the National Institute of Standards and Technology (NIST) while rutile TiO<sub>2</sub>-NPs  
14 were purchased from Sigma (St. Louis, MO, USA). The brookite TiO<sub>2</sub>-NPs were synthesized at  
15 the U.S. Environmental Protection Agency's (EPA's) Andrew W Breidenbach Environmental  
16 Research Center (AWBERC) located in Cincinnati, Ohio. The brookite synthesis method has  
17 been described in previous studies.<sup>26-27</sup> In brief, an aliquot of 28.5 g of TiCl<sub>4</sub> was dissolved in  
18 50 mL concentrated HCl at room temperature to yield a light yellow solution. The acidified  
19 TiCl<sub>4</sub> solution was slowly diluted with 450 mL distilled water and then 1 L of isopropanol was  
20 added to the diluted solution. The mixture was then refluxed for 20 hours at 80 °C to obtain a  
21 homogeneous milky white solution, which was centrifuged, decanted, and air dried. Solids were  
22 analyzed as-prepared without further washing or purification. The three selected TiO<sub>2</sub>-NPs were  
23 characterized before and after heat and pressure treatment. The X-ray diffraction (XRD) was

1 performed using a PANAnalytical X'pert Pro 2 $\theta$  diffractometer operating in the reflection mode  
2 with Cu-K $\alpha$  radiation (45 kV, 40 mA) and a step scan mode over the range of 10 to 90 $^\circ$ .  
3 Diffraction patterns for each TiO $_2$ -NP polymorph were compared with reference patterns from  
4 the Joint Committee on Powder Diffraction Standards (JCPDS) database. Brunauer-Emmett-  
5 Teller (BET) surface area measurements of heat and pressure treated and untreated TiO $_2$ -NPs  
6 were determined using a Tristar 3000 (Micromeritics, GA, USA) porosimeter analyzer after  
7 purging with N $_2$  gas for 2 hrs at 150  $^\circ$ C. Transmission Electron Microscopy (TEM) was used to  
8 determine the sizes and the shapes of all three TiO $_2$ -NPs polymorphs before and after  
9 heat/pressure treatment. A JEOL-2100 STEM (JEOL Inc., USA) with a side mounted Gatan  
10 digital camera was used for imaging TiO $_2$ -NPs. Titanium dioxide samples were prepared by  
11 depositing 15  $\mu$ L of TiO $_2$ -NPs dispersed water suspension on a formvar-carbon coated copper  
12 grid. Samples were air-dried at room temperature overnight in a dust-free box. Images were  
13 captured at an accelerating voltage of 200 kV, and collected using Gatan software.

14

### 15 **Environmental matrices used for TiO $_2$ -NP spikes**

16

17 River sediment, bentonite and kaolinite were used as environmental matrices. These materials  
18 were digested with and without additions of the three polymorph TiO $_2$ -NPs to determine the  
19 background Ti concentrations and Ti spike recoveries. River sediment was collected from  
20 experimental stream beds at EPA's Experimental Stream Facility (ESF) located in Milford, Ohio.  
21 Plastic trays with porous side walls and a solid base were used to collect the river sediment and  
22 processed as follows: A 250  $\mu$ m sieve was placed on top of a 20 L plastic container and the  
23 sample was wet sieved. The sieved material, which was collected in 20 L containers, was

1 allowed to settle for 5 days. After 5 days, the bottom sediment layer was collected by siphoning  
2 out the supernatant prior to drying in an oven at 105 °C for 5-7 days. The dried sediment sample  
3 was then gently crushed using mortar and pestle and again passed through a 250 µm sieve.<sup>26</sup>

4  
5 The kaolinite (1:1) and bentonite (2:1) clay minerals were purchased from Sigma Chemical  
6 Company (St. Louis, MO, USA). Three sets of TiO<sub>2</sub>-NP-spiked samples were prepared from  
7 each environmental matrix separately. In a glove box, ten grams of each environmental matrix  
8 were spread evenly on aluminum foil and 0.2 g of each TiO<sub>2</sub>-NP type was sprinkled uniformly to  
9 achieve a 2% TiO<sub>2</sub>-NP spiking rate on the basis of TiO<sub>2</sub> or 1.2% Ti. While 2% TiO<sub>2</sub>-NP spiking  
10 samples were used for digestion, a separate set of 5% TiO<sub>2</sub>-NP-spiked samples were also  
11 prepared for XRD analysis. It is highly unlikely to find high Ti concentrations in conventional  
12 environmental samples, but these spike rates were required to achieve uniform distribution of  
13 TiO<sub>2</sub>-NP in samples for digestion and polymorph determination. For example, the XRD analysis  
14 requires a minimum of 5% analyte for consistent and repeatable results. Each mixture was then  
15 transferred to separate sampling bottles and mixed for 30 minutes using an end-over-end rotator  
16 (Rotamix, ATR Inc. Laurel, MD, USA). A portion of environmental material with and without  
17 spiked TiO<sub>2</sub>-NPs was heat/pressure treated (described in section 2.5). The dissolution efficacy of  
18 TiO<sub>2</sub>-NPs with and without environmental materials was tested using MW-based HF mixed acid  
19 and MF-based KOH digestion techniques. The background Ti concentrations of the  
20 environmental materials were used in the calculation of Ti-spike recoveries.

21

22 **HNO<sub>3</sub>/ HF mixed acids microwave digestion**

23

1 In the mixed acid digestion method,  $0.25 \pm 0.001$  g of pure  $\text{TiO}_2$ -NPs,  $0.25 \pm 0.001$  g of  
2 environmental material and  $0.25 \pm 0.001$  g of  $\text{TiO}_2$ -NPs-blended environmental material were  
3 digested separately in triplicate using a mixture of HF (3 mL) and  $\text{HNO}_3$  (9 mL) following EPA  
4 Method 3052.<sup>28</sup> Each sample solution was diluted to 100 mL using nano-pure water and was  
5 transferred to acid-washed ( $\text{HNO}_3$ ), triple-rinsed (de-ionized  $\text{H}_2\text{O}$ ) plastic bottles and stored at  
6  $4^\circ\text{C}$  prior to analysis.

### 8 **KOH alkaline MF fusion**

9  
10 To be consistent with the mixed acid digestion method, the same amount of  $\text{TiO}_2$ -NPs, and  
11 environmental materials with and without spiked  $\text{TiO}_2$ -NPs were digested with 1.6 g KOH in  
12 nickel crucibles in triplicate. Fusion was performed using a pre-heated Lindberg MF (Riverside,  
13 MI, USA) at  $700^\circ\text{C}$  for 20 minutes.<sup>26</sup> After 20 minutes, fused samples were allowed to cool to  
14 room temperature, and nano-pure water was added to dissolve the solidified fusion mixture.  
15 Similar to the standard fusion technique, the fusion mixture was brought up to 250 mL using  
16 nano-pure water after adding 50 mL of 50% HCl solution and 0.5 g of oxalic acid. Samples were  
17 immediately analyzed for total Ti content or stored at  $4^\circ\text{C}$  until analysis.<sup>29</sup>

### 18 **Heat and pressure effects on Ti recovery from environmental matrices**

19  
20 Portions of  $\text{TiO}_2$ -NPs, environmental materials with and without spiked  $\text{TiO}_2$ -NPs, were treated  
21 in triplicate at constant heat ( $300^\circ\text{C}$ ) and pressure (10.3 bar) for 4 hours to evaluate the effects of  
22 heat and pressure on the stability and reactivity of  $\text{TiO}_2$ -NPs. A series of stainless-steel reaction

1 vessels (50 ml, Pressure Products Industries, Warminster, PI) maintained at aforementioned  
2 conditions were used to treat the samples. The vessel temperatures were kept at set condition  
3 using Duo-Thermo-O-Watch (Glass-Col,) equipped with digital thermocouple, while the vessel  
4 pressures were monitored using digital pressure controllers (Omega Engineering, Inc.). Natural  
5 air was used to pressurize the reactor system when heat was nearing preset values. Heat and  
6 pressure treated samples were removed and characterized prior to digestion as described  
7 previously.

8

### 9 **Sample and data analysis**

10

11 The total Ti concentration was measured using a PerkinElmer 2300 DV inductively coupled  
12 plasma-optical emission spectrometer (ICP-OES). Prior to analyses for Ti, the total dissolved  
13 solids (TDS) content of alkaline fused samples was determined using standard American Public  
14 Health Association (APHA) methods,<sup>30</sup> and samples were diluted to reduce TDS content. All  
15 acids (HNO<sub>3</sub>, HF and HCl) were of trace metal grade and nano-pure water ( $\geq 18 \mu\Omega \text{ cm}^{-1}$   
16 resistivity) was obtained from a Nanopure™ (Barnstead Thermo Scientific, Dubuque, IA, USA)  
17 water purification system. An ICP single-element Ti standard solution (Spex Cetriprep,  
18 Metuchen, NJ, USA) of 1000 mg L<sup>-1</sup> was diluted as needed for calibration and internal quality  
19 checks. A diluted ICP multi-element standard solution of 1000 mg L<sup>-1</sup> (AccuStandard, New  
20 Haven, CT, USA) was used as an external standard for calibration verification. In order to  
21 overcome the matrix effects, matrix-matched standards were used for calibration. Titanium  
22 concentrations were determined in all three environmental materials, TiO<sub>2</sub>-NP-spiked  
23 environmental materials and pure TiO<sub>2</sub>-NPs.

1  
2 To distinguish the effect of heat-pressure on TiO<sub>2</sub>-NP polymorphs stability or dissolution, data  
3 for each digestion were analyzed separately using analysis of variance (ANOVA). Significant  
4 differences among means were determined using protected Fisher's least significant different  
5 test, only when ANOVA indicated significant differences. The SYSTAT (Systat for Windows,  
6 version 11) program was used to perform statistical analyses.

## 7 **Results and discussion**

### 8 **Characterization of pure Ti-NPs**

9  
10  
11  
12 The XRD patterns for the three Ti-NP polymorphs exhibited strong diffraction patterns  
13 consistent with standard JCPDS diffraction for anatase (01-086-1157), brookite (01-075-1582)  
14 and rutile (01-075-1750) (Fig. 1a-c). Diffraction patterns of both anatase and brookite TiO<sub>2</sub>-NPs  
15 exhibited a decrease in the peak width at half max and an increase in intensity after exposing to  
16 heat and pressure (Fig. 1a and b). However, diffraction peak positions of both polymorphs were  
17 similar before and after exposing to heat and pressure. The diffraction peak shapes of untreated  
18 rutile TiO<sub>2</sub>-NPs were comparatively narrower than the anatase and brookite TiO<sub>2</sub>-NPs. In  
19 addition, rutile diffraction peak shape did not change after exposing to heat and pressure,  
20 suggesting a well-defined stable crystalline structure in the rutile TiO<sub>2</sub>-NPs (Fig. 1c). The BET  
21 surface area of rutile polymorph TiO<sub>2</sub>-NPs before heat and pressure exposure is approximately 1  
22 m<sup>2</sup> g<sup>-1</sup> and about 159 and 203 times smaller than anatase and brookite polymorphs, respectively  
23 (Table 1). This large difference in surface area could be attributed to larger particle size or

1 aggregation of the rutile TiO<sub>2</sub>-NPs. The surface area of rutile polymorph TiO<sub>2</sub>-NPs increased  
2 marginally after exposing to heat and pressure. The surface area of anatase 159 m<sup>2</sup> g<sup>-1</sup> and  
3 brookite 204 m<sup>2</sup> g<sup>-1</sup> before heat and pressure treatment reduced to 66 and 37 m<sup>2</sup> g<sup>-1</sup>, respectively,  
4 after exposing to heat and pressure (Table 1). Particle size measurements by TEM images (Fig.  
5 2) for the three pure polymorphs are in agreement with that of surface area. For example, the  
6 TEM-measured anatase and brookite TiO<sub>2</sub>-NPs ranged from 2-5 nm prior to heat and pressure  
7 treatment (Fig. 2 a and c). The image for rutile TiO<sub>2</sub>-NPs before heat and pressure treatment  
8 showed comparatively bigger particle aggregate ranging between 25-50 nm (Fig. 2e). Both  
9 anatase and brookite TiO<sub>2</sub>-NPs exhibited a clear aggregation after heat and pressure treatment  
10 (Fig. 2 b and d). The changes in rutile TiO<sub>2</sub>-NPs particle size after heat and pressure were not  
11 apparent in TEM images but did not show detectable crystal growth. To verify the impact of heat  
12 and pressure treatment, the crystallite sizes were estimated for anatase and brookite polymorphs  
13 from XRD patterns using Scherrer equation (Table 2). The lack of variability between treated  
14 and untreated rutile XRD patterns prevented estimating rutile polymorph size. It was observed  
15 that brookite polymorph sample contained both anatase and rutile polymorphs (Table 2), and  
16 rutile particle size in brookite sample increased due to heat and pressure treatment. The peaks  
17 corresponding to anatase (101) plane, rutile (110) plane, and brookite (121) plane were used to  
18 calculate the sizes. The particle size estimated using XRD patterns are in line with the TEM  
19 particle size.

20

21

22 **Effect of digestion type on different polymorphs of TiO<sub>2</sub>-NPs with and without**  
23 **environmental matrices**

1  
2 The concentration of Ti in the blank was below the instrument method detection limit of 0.45  $\mu\text{g}$   
3  $\text{L}^{-1}$  and none of the reagents used contained any detectable concentration of Ti indicating that  
4 measured concentration of Ti was associated to the samples (Tables 3 and 4). Amount of Ti in  
5 the environmental matrices was subtracted to determine the percent Ti recovery from  $\text{TiO}_2$ -NPs  
6 when  $\text{TiO}_2$ -NP polymorphs were blended in environmental matrices. Of the three environmental  
7 matrices, the kaolinite contained the highest Ti content ( $\sim 8 \text{ mg g}^{-1}$ ) which is about two-fold  
8 greater than the sediment Ti content. The bentonite clay contained around  $1 \text{ mg g}^{-1}$  of Ti. Both  
9 digestion techniques resulted in similar Ti concentrations for the two clay materials before heat  
10 and pressure treatment. In contrast, mixed acid digestion resulted in comparatively lower Ti  
11 concentration than the KOH fusion from sediments (Table 3).

12  
13 Titanium percent recoveries for  $\text{TiO}_2$ -NPs in anatase form was  $80 (\pm 14.0)$  and for brookite form  
14 was  $81 (\pm 3)$ , by the MW-based  $\text{HF}/\text{HNO}_3$  mixed acid digestion procedure. The corresponding  
15 percent recoveries were  $96 (\pm 2)$  and  $85 (\pm 2)$  by MF-based KOH fusion. In contrast, the Ti  
16 percent recovery of  $14 (\pm 1)$  for pure rutile  $\text{TiO}_2$ -NPs by the MW-based  $\text{HF}/\text{HNO}_3$  mixed acid  
17 digestion was significantly lower than  $87 (\pm 5)$  by MF-based KOH fusion (Ti concentration for  
18 pure  $\text{TiO}_2$ -NPs are not presented). Similarly, the percent Ti recoveries for rutile polymorph  
19 when blended in the environmental matrices were significantly lower by MW-based  $\text{HF}/\text{HNO}_3$   
20 mixed acid digestion compared to MF-based KOH fusion (Fig. 3). Both anatase and brookite  
21 resulted in similar Ti recoveries when blended in the environmental matrices regardless of the  
22 method of digestion. Relatively higher variability was observed for anatase in sediments under  
23 mixed acid digestion before treatment (Fig. 3), which could be a result of uneven dispersion of



1 applied TiO<sub>2</sub>-NPs in three replicates.<sup>26</sup> The experimental results show that MW-based HF/HNO<sub>3</sub>  
2 acids digestibility may not be an effective technique to dissolve rutile TiO<sub>2</sub>-NPs either in pure  
3 form or blended in environmental materials. These results reveal that the type of TiO<sub>2</sub>-NP  
4 polymorph present in the environmental samples can influence recovery of Ti under different  
5 digestion techniques. It is recommended that the KOH fusion technique be used to determine the  
6 amount of Ti present in unknown environmental samples.

7  
8 The chemical reactions and thermodynamic properties of reactants are complex during the  
9 mineral digestion process and have not yet been clearly identified.<sup>24</sup> However, alkali  
10 compounds have been reported as metal (including refractory metal Ti) recovery enhancing  
11 compounds.<sup>24</sup> The spontaneous formation and dissolution of oxide films in the presence of  
12 strong alkaline electrolytes (KOH) are the possible reasons for higher Ti recoveries by MF-based  
13 KOH fusion.<sup>25</sup> The rate of dissolution of oxide films formed on the surface of TiO<sub>2</sub>-NPs in the  
14 presence of the strong acid solution is slower, and low recovery of thermodynamically stable  
15 rutile TiO<sub>2</sub>-NPs by HF/HNO<sub>3</sub> mixed acids in the current study is consistent with the literature.<sup>12</sup>  
16 However, the deviation of anatase and brookite TiO<sub>2</sub>-NPs from the same trend, indicated that  
17 HF/HNO<sub>3</sub> mixed acid digestion may not be a poor dissolution technique across all polymorphs of  
18 TiO<sub>2</sub>-NPs as previously noted,<sup>16,18</sup> but dissolution appears to be polymorph crystal structure-  
19 dependent (Table 4).

20

21 **Effect of heat and pressure on different polymorphs of TiO<sub>2</sub> mineral digestion**

22

1 The heat and pressure treatment resulted in a decrease in the percent Ti recoveries across all  
2 TiO<sub>2</sub>-NP-blended environment matrices by HF/HNO<sub>3</sub> acid digestion (Fig. 3). In contrast, percent  
3 Ti recoveries increased when the heat and pressure treated TiO<sub>2</sub>-NP-blended environment  
4 matrices were KOH digested (Fig. 3). The decreased Ti recoveries in the HF/HNO<sub>3</sub> digestion  
5 were more prominent for the anatase and brookite polymorphs than rutile. Previous research  
6 revealed that nano-scale anatase and brookite polymorphs may alter phase stability and transfer  
7 to rutile when heated.<sup>16,22</sup> For example, Smith et al.<sup>31</sup> revealed that the transformation of anatase  
8 to rutile is thermodynamically favorable at all temperatures between 0 and 1,300 K on the basis  
9 of Gibbs free energy calculations. However, others reported that conversion of anatase and  
10 brookite to rutile only occurred at temperature ranges between 800-1,023 K, much greater than  
11 the 573 K in the current experiment.<sup>32</sup> Therefore, the lower recoveries for Ti in the heat and  
12 pressure treated TiO<sub>2</sub>-NP-environment materials from HF/HNO<sub>3</sub> digestion may not be an effect  
13 of phase transformation, rather an increase in particle-particle interaction and/or particle  
14 aggregation of anatase and brookite compared to rutile (Fig. 2). Even low heating under pressure  
15 has a profound effect on particle interaction and aggregation of anatase and brookite TiO<sub>2</sub>-NP as  
16 illustrated by a reduction in the peak width and half max and an increase in the kurtosis of the  
17 diffraction peaks.<sup>20</sup> This was apparent by the XRD peak positions of anatase and brookite before  
18 and after heat (300 °C)/pressure (10.3 bar) treatment in the current experiment (Fig. 1). The  
19 impact of heat and temperature on digestion technique was not only confined to TiO<sub>2</sub>-NPs but  
20 also to the environmental matrices (Table 3). Similar to TiO<sub>2</sub>-NPs, Ti concentrations of  
21 environmental matrices declined for the MW-based mixed acid digestion while the opposite  
22 occurred for the MF-based KOH fusion after exposing to heat and pressure treatment.

23

1 The particle reaction-limited aggregation may have resulted in a surface area reduction of 58%  
2 and 82% for anatase and brookite, respectively, after heat and pressure treatment (Table 1). In  
3 contrast to the two aforementioned types of TiO<sub>2</sub>-NP polymorphs, diffraction peaks of rutile did  
4 not change after heat and pressure treatment, indicating a stable crystal structure of rutile (Fig.  
5 2). This is in agreement with the subtle change in surface area of rutile after the heat and  
6 pressure treatment.

7  
8 The change of surface properties of TiO<sub>2</sub> polymorphs due to heat and pressure treatment may  
9 have altered the surface enthalpy and the stability in the order of anatase > brookite > rutile.<sup>20</sup>  
10 Additionally, the thermodynamic stability is particle size dependent, and anatase is  
11 thermodynamically stable at smaller size, brookite at intermediate sizes and rutile at the largest  
12 sizes.<sup>20,22</sup> The XRD results (Table 2 and Fig. 2) clearly indicate that heat and pressure treatment  
13 results in phase transformations where the anatase and brookite polymorphs are converted to a  
14 more stable rutile form. These phase transformations combined with the particle disaggregation  
15 in the presence of KOH may have resulted in greater recovery of Ti by MF-based KOH fusion.  
16 The growth in particle size due to reaction-limited aggregation of anatase and brookite (Table 2  
17 and Fig. 2), may have decreased the Ti released by the MW-based HF digestion similar to rutile.

## 18 19 **Conclusions**

20  
21 Experimental results reveal that the digestibility of TiO<sub>2</sub>-NPs is more closely associated with the  
22 particle aggregation and TiO<sub>2</sub>-NP polymorphs. At the spiked levels studied, the HF/HNO<sub>3</sub> acids  
23 digestibility of TiO<sub>2</sub>-NPs is polymorph dependent while MF-based KOH digestibility is

1 polymorph independent. The HF/HNO<sub>3</sub> acids digestibility was impaired by greater aggregation  
2 whereas MF-based KOH digestibility was not affected by the degree of particle aggregation  
3 and/or crystallization. The use of heat and pressure treatment considerably influenced the  
4 particle characteristics and surface properties of TiO<sub>2</sub>-NPs. The aggregation mechanism has an  
5 effect on surface enthalpy. The dissolution efficacy of HF further diminished with increasing  
6 aggregation of the TiO<sub>2</sub>-NP polymorphs. In contrast, the dissolution capacity of aggregated  
7 TiO<sub>2</sub>-NP polymorphs further increased by KOH fusion. Thus, KOH can be used to dissolve all  
8 three TiO<sub>2</sub>-NP polymorphs evaluated in this study while HF is only effective for anatase and  
9 brookite dissolution. Further studies are necessary to verify the trends observed in this  
10 experiment at a lower environmentally relevant concentrations. These results provide useful  
11 information for the selection of digestion techniques to determine Ti content in TiO<sub>2</sub>-NP  
12 contaminated environmental samples.

13

#### 14 **Acknowledgements**

15

16 The authors would like to thank Timothy Kling and Nancy Shaw of CB&I Federal Services LLC  
17 for their help with the laboratory work. The U.S. Environmental Protection Agency, through its  
18 Office of Research and Development's National Risk Management Research Laboratory, funded  
19 and managed, or partially funded and collaborated in, the research described herein. It has been  
20 subjected to the Agency's administrative review and has been approved for external publication.  
21 Any opinions expressed in this paper are those of the author (s) and do not necessarily reflect the  
22 views of the Agency, therefore, no official endorsement should be inferred. Any mention of trade  
23 names or commercial products does not constitute endorsement or recommendation for use.

1  
2  
3  
4  
5  
6  
7  
8  
9  
10  
11  
12  
13  
14  
15  
16  
17  
18  
19  
20  
21  
22

### **Notice**

*The U.S. Environmental Protection Agency, through its Office of Research and Development, funded and managed, or partially funded and collaborated in, the research described herein. It has been subjected to the Agency's administrative review and has been approved for external publication. Any opinions expressed in this paper are those of the author(s) and do not necessarily reflect the views of the Agency, therefore, no official endorsement should be inferred. Any mention of trade names or commercial products does not constitute endorsement or recommendation for use.*

### **References**

1. X. Fujishima and C.R. Zhang, *Chimie*, 2006, **9**, 750-760.
2. M.R. Hoffmann, S.T. Martin, W.Y. Choi and D.W. Bahnemann, *Chem. Rev.*, 1995, **95**, 69-96.

- 1 3. B. Trouiller, R. Reliene, A. Westbrook, P. Solaimani and R.H. Schiestl, *Cancer Res.*, 2009,  
2 **69**, 8784-8789.
- 3
- 4 4. A.L. Linsebigler, G.Q. Lu and J.T. Yates, *Chem. Rev.*, 1995, **95**, 735-758.
- 5
- 6 5. D.A. Tryk, A. Fujishima and K. Honda, *Electrochim. Acta.*, 2000, **45**, 2363-2376.
- 7
- 8 6. A. Zaleska A, *Rec. Pat. Engi.*, 2008, **2**, 157-164.
- 9
- 10 7. International Agency for Research on Cancer, 2010, **93**, pp 754.
- 11
- 12 8. M. Balcerzak, *Anal. Sci.*, 2002, **18**, 737-750.
- 13
- 14 9. M.G.A. Korn, A.C. Ferreira, A.C.S. Costa, J.A. Nobrega and C.R. Silva, *Microchem. J.*,  
15 2002, **71**, 41-48.
- 16
- 17 10. A.S.M. Madeja and W. Mulak, *J. Hazard. Mater.*, 2009, **164**, 776-780.
- 18
- 19 11. A.P. Packer, D. Lariviere, C. Li, M. Chen, A. Fawcett, K. Nielsen, K. Mattson, A. Chatt, C.  
20 Scriver and L.S. Erhardt, *Anal. Chim. Acta.*, 2007, **588**, 166-172.
- 21
- 22 12. K.S. Patel, P.C. Sharma and P. Hoffmann, *Fresenius' J. Anal. Chem.*, 2000, **367**, 738-741.
- 23

- 1 13. P. Roy, V. Balaram, A. Bhattacharaya, P. Nasipuri and M. Satyanarayanan, *Curr. Sci.*, 2007,  
2 **93**, 1122-1126.
- 3
- 4 14. I. Tressl, O. Mestec and M. Suchanek, *Chem. Commun.*, 2000, **65**, 1875-1887.
- 5
- 6 15. S. Uchida, K. Tagami and K. Tabei, *Anal. Chim. Acta.*, 2005, **535**, 317-323.
- 7
- 8 16. J. Sanchez, N Marino, M.C. Vaquero, J. Ansorena and I. Legorburu, *Water Air Soil Pollut.*,  
9 1998, **107**, 303-319.
- 10
- 11 17. V.F. Taylor, A. Toms and H.P. Longerich, *Anal. Bioanal. Chem.*, 2002, **372**, 360-365.
- 12
- 13 18. C. Yafa and J.G. Farmer, *Anal. Chim. Acta.*, 2006, **557**, 296-303.
- 14
- 15 19. F. Dachille, P.Y. Simons and R. Roy, *Amri. Mineral*, 1968, **53**, 1929-1939.
- 16
- 17 20. T.J. Park, A. Levchenko, H. Zhou, S. Wong and A. Navrotsky, *J. Mater. Chem.*, 2010, **20**,  
18 8639-8645A.
- 19
- 20 21. T. Mitsuhashi and O.J. Kleppa, *J. Am. Ceram. Soc.*, 1979, **62**, 356-357.
- 21
- 22 22. H. Zhang and J.F. Banfield, *J. Mater. Chem.*, 1998, **8**, 2073-2076.
- 23

- 1 23. S.J. Palmer, R.L. Frost and T. Nguyen, *Coord. Chem. Revs.*, 2009, **253**, 250-267.
- 2
- 3 24. L.Xiao-bin, F. Wei-an, Z. Qiu-sheng, L. Gui-hua and P. Zhi-hong, *Trans. Nonferrous Met.*
- 4 *Soc. China*, 2010, **20**, 142-146.
- 5
- 6 25. A. Prusi, L. Arsov, B. Haran and B. Popov, *J. Electrochem. Soc.*, 2002, **149**, B491-B498.
- 7
- 8 26. R.G. Silva, M.N. Nadagouda, J. Webster, S. Govindaswamy, K.D. Hristovski, R.G. Ford, C.
- 9 Patterson and C.A. Impellitteri, *Environ. Sci. Processes Impacts*, 2013, **15**, 645-652.
- 10
- 11 27. B.I. Lee, X. Wang, R. Bhave and M. Hu, *Materials Letters* 2006, **60**, 1179–1183.
- 12
- 13 28. USEPA Method 3052: Microwave assisted acid digestion of siliceous and organically based
- 14 matrices 2nd ed. *Test Methods for Evaluating Solid Waste, Physical/Chemical Methods*; U.S.
- 15 Government Printing Office: Washington, DC, 1997.
- 16
- 17 29. ASTM, Designation: C1463-00 (Reapproved 2007), West Conshohocken, PA, USA, 2007.
- 18
- 19 30. APHA-AWWA-WPCF, *Standard Methods for the Examination of Water and Wastewater*,
- 20 20th edition, American Public Health Association Washington D.C., USA, 1998.
- 21
- 22 31. S.J. Smith, R. Stevens, S. Liu, G. Li, A. Navrotsky, J. Boerio-Goates, and B.F. Woodfield,
- 23 *Ameri. Mineralog.*, 2009, **94**, 236-243.



1

2 32. H. Zhang and J.F. Banfield, J. Phys. Chem., 2000, **8**, 3481-3487.

3

4

5

6

7

8

9

10

11

12

13

14

15

16

17 **Table and Figure Captions**18 Table 1 Characteristics of TiO<sub>2</sub>-NPs before and after heat and pressure treatments

19 Table 2 Particle size estimation from XRD using Scherrer equation

20 Table 3 Concentration (mg g<sup>-1</sup>) of Ti in sediments, kaolinite and bentonite before and after heat  
21 and pressure treatment determined by ICP-OES using MW-based HF/HNO<sub>3</sub> acids and MF-based  
22 KOH fusion digestions

1 Table 4 Concentration ( $\text{mg g}^{-1}$ ) and percent recovery of Ti in  $\text{TiO}_2$ -NP-spiked sediment,  
2 kaolinite, and bentonite by ICP-OES using MF-based KOH fusion and MW-based HF/ $\text{HNO}_3$   
3 acids before and after heat and pressure treatments.

4

5

6 Figure 1 XRD patterns of anatase (a), brookite (b) and rutile (c)  $\text{TiO}_2$ -NPs before and after heat  
7 and pressure treatment.

8

9 Figure 2 TEM images for anatase (a and b), brookite (c and d) and rutile (e and f)  $\text{TiO}_2$ -NPs  
10 before and after heat and pressure treatment, respectively.

11

12 Figure 3 Percent recovery of Ti as a function of polymorph and digestion technique before and  
13 after heat and pressure treatment. The letters along the top of the figure indicate the specific  
14 sample. The first letter indicates the  $\text{TiO}_2$  polymorph: A = Anatase, B= Brookite, R=Rutile.  
15 The second letter indicates the environmental matrix: S = Sediment, K=Kaolin, B = Bentonite.

Table 1

Material	Source	Surface area before (m <sup>2</sup> g <sup>-1</sup> )	Surface area after (m <sup>2</sup> g <sup>-1</sup> )
TiO <sub>2</sub> -Anatase	NIST	158.8	66.4
TiO <sub>2</sub> -Brookite	Prepared	203.5	36.9
TiO <sub>2</sub> -Rutile	Sigma Aldrich	0.9	1.3

Table 2.

XRD pattern	Heat/Pressure	Anatase	Brookite	Rutile
Fig 1A	Untreated	5.4 nm (diff. 2θ=1.5)		
	Treated	9.0 nm (diff. 2θ=0.9)		
Fig 1B	Untreated	3.8 nm (diff. 2θ=2.1)	11.6 nm (diff. 2θ=0.7)	11.6 nm(diff. 2θ=0.7)
	Treated	26.9 nm (diff. 2θ=0.3)	40.8 nm (diff. 2θ=0.2)	20.2 nm(diff. 2θ=0.4)

Table 3

Material	Ti concentration mg g <sup>-1</sup> (±SD) MW-based HF/HNO <sub>3</sub> digestion		Ti concentration mg g <sup>-1</sup> (±SD) MF-based KOH fusion	
	before	After	before	after
	Sediment	3.0 (±0.1)	2.5 (±0.0)	4.2 (±0.0)
Kaolin	8.1 (±0.1)	6.9 (±0.1)	8.0 (±0.4)	9.2 (±0.3)
Bentonite	1.0 (±0.0)	0.5 (±0.0)	1.0 (±0.1)	2.9 (±0.0)

Data in parentheses are ± standard deviation (SD) of mean

Table 4

TiO <sub>2</sub> -NP polymorphs	Environmental Material	Heat/Pressure Treatment	Acid extracted concentration mg g <sup>-1</sup>	Ti Alkali fusion concentration mg g <sup>-1</sup>
Anatase	Sediment	Untreated	19.2a	13.6a
		Treated	8.4b	19.1b
Anatase	Sediment	Untreated	15.0a	16.0a
		Treated	13.4a	17.5a
Anatase	Bentonite	Untreated	10.9a	10.6a
		Treated	7.3b	13.7b
Brookite	Sediment	Untreated	15.0a	13.0a
		Treated	6.1b	16.0b
Brookite	Kaolin	Untreated	14.2a	13.2a
		Treated	7.5b	21.1b
Brookite	Bentonite	Untreated	8.8a	8.8a
		Treated	6.7a	11.9b
Rutile	Sediment	Untreated	5.9a	13.2a
		Treated	2.6b	18.6b
Rutile	Kaolin	Untreated	9.5a	14.4a
		Treated	5.2b	20.8b
Rutile	Bentonite	Untreated	2.3a	10.1a
		Treated	1.2a	13.8b

Data followed by the same letter for a polymorph/environmental material mixture within a digestion method are not significantly different at p 0.05.

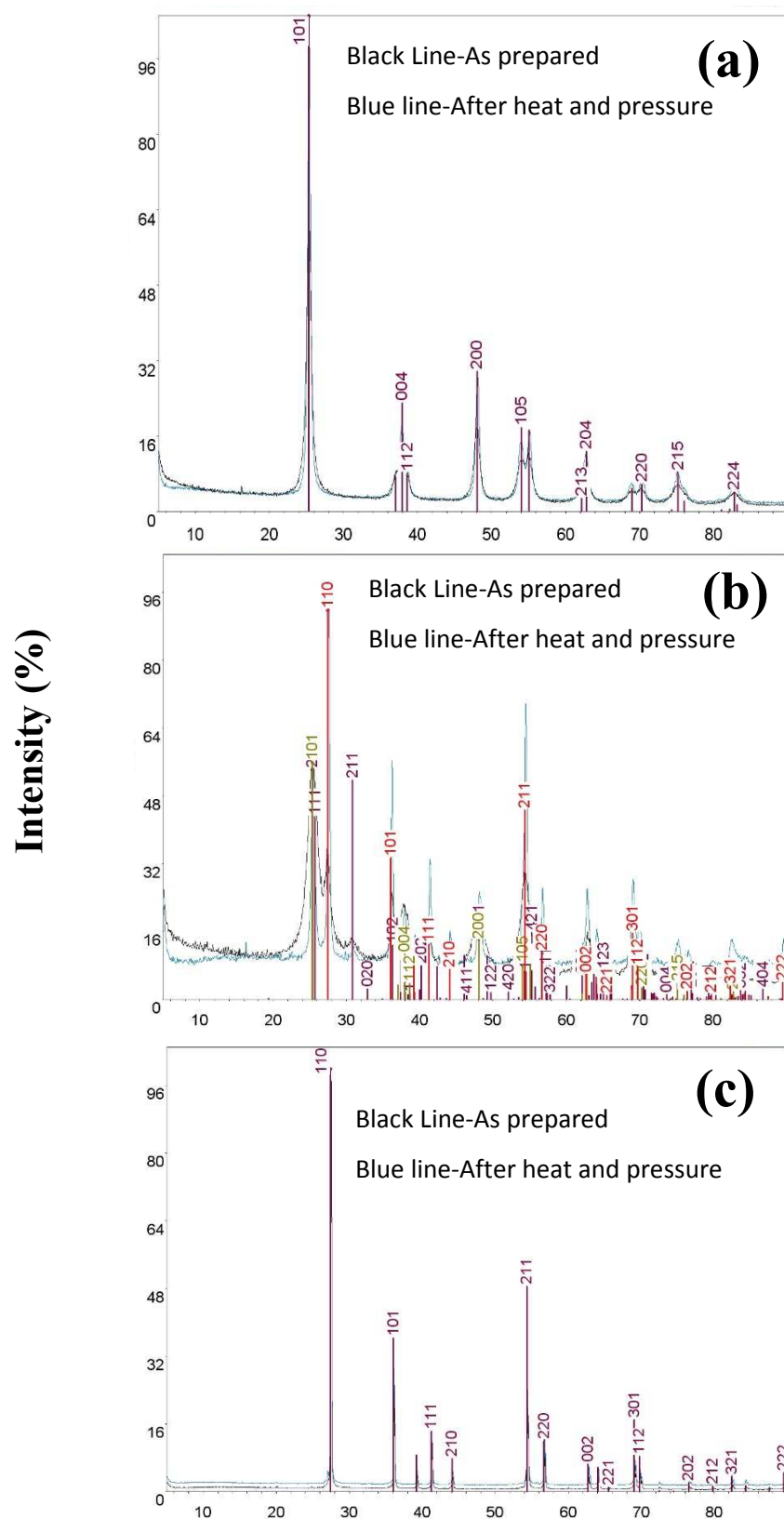
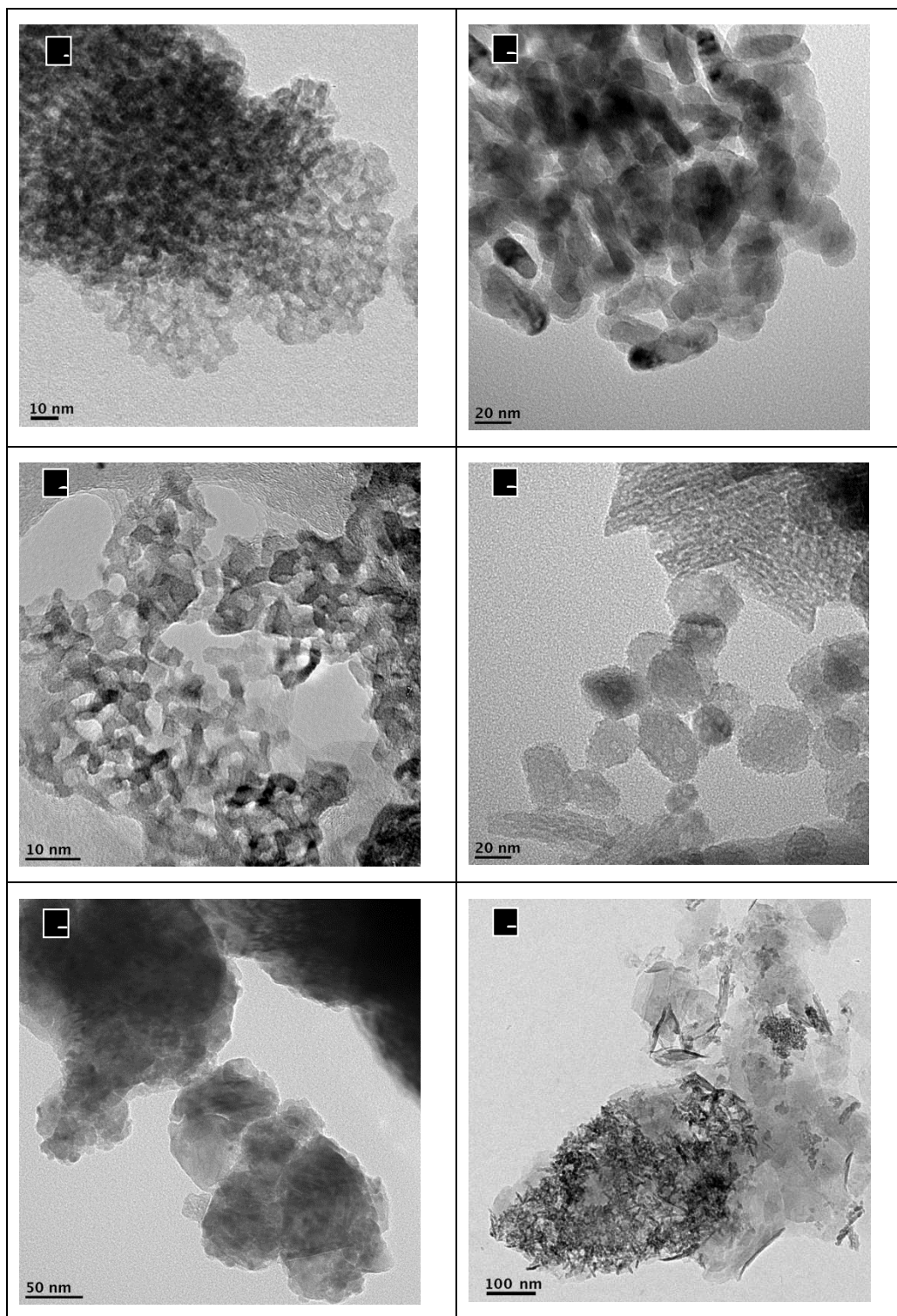


Figure 1



Anatase TiO<sub>2</sub>-NPs untreated (A) and temperature and pressure treated (B)  
Brookite TiO<sub>2</sub>-NPs untreated (C) and temperature and pressure treated (D)  
Rutile TiO<sub>2</sub>-NPs untreated (E) and temperature and pressure treated (F)

Figure 2

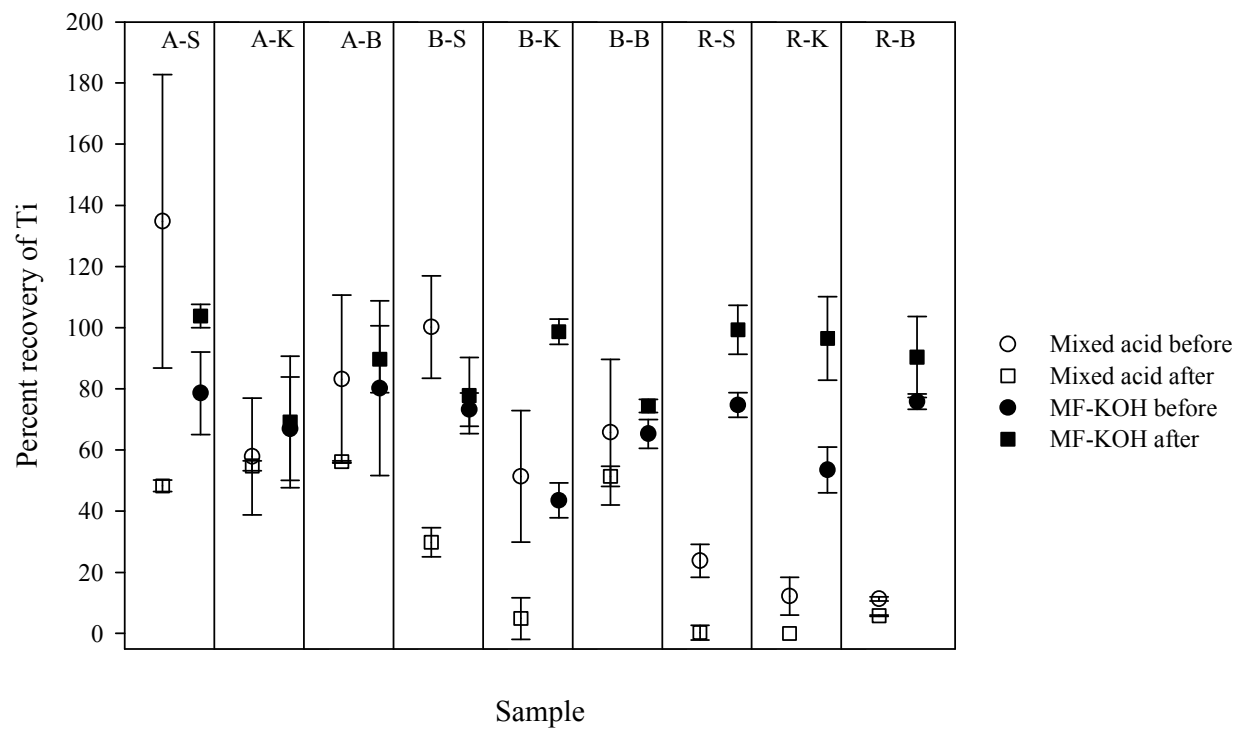


Figure 3